Hysteresis loss and stochastic resonance: A numerical study of a double-well potential

Mangal C. Mahato* and Subodh R. Shenoy
School of Physics, University of Hyderabad, Hyderabad 500 134, India
(Received 14 February 1994)

A Langevin dynamic simulation is carried out in order to understand the phenomena of hysteresis in a double-well system represented by a Landau (m^4) potential, where m is the order parameter, with a symmetrical sawtooth-type periodic external field. The calculation of a hysteresis loop is based on the statistics of first-passage time to make a transition from one well to the other across the potential barrier as the external field (of symmetrical sawtooth type) is swept in time. The basic construction of our model used to understand hysteresis rules out any dynamical (symmetry breaking) phase transition predicted by other workers in Ising- and O($N\rightarrow\infty$)-model systems. Also, we do not find any universal scaling relationship between the hysteresis loss and the field-sweep "frequency." Our treatment, however, makes close contact with a recently observed phenomenon of stochastic resonance: the hysteresis loss shows a stochastic resonant behavior with respect to the noise strength. We discuss the recent experiment on the observation of the Kramers rate and stochastic resonance by Simon and Libchaber [Phys. Rev. Lett. **68**, 3375 (1992)] in light of our results.

PACS number(s): 02.50.Ey, 42.65.Vh, 75.60.Ej

I. INTRODUCTION

Hysteresis is a kinetic phenomenon. The phenomenon is a signature of how the system parameters respond to an external field sweep. The most familiar example of hysteresis is the curve of magnetization M versus the external magnetic field H. The nonlinear and delayed response M to the external field H is characteristic of hysteresis in many systems with different measured physical quantities M and corresponding different fields H. The simple minded reason for the occurrence of the phenomenon is that the system spends time in its metastable state (accumulated strain) before it jumps (sudden relaxation) to the stable state appropriate to the external field. The process of jumping across the dividing potential barrier between the metastable and the stable state is most often accompanied by frictional losses (nonequilibrium process) and consequently the irreversibility of the curve as the field is reversed is natural. The frictional loss depends on various factors including the rate at which the external field is being swept. This kinetic aspect of the hysteresis phenomenon, however, was not given due attention till recently, even though the concept of hysteresis formally originated more than a century ago [1]. The present work is directed toward supplementing the understanding (which is far from complete) of hysteresis as a kinetic phenomenon and of its relation to the recently discovered phenomenon of stochastic resonance (to be explained below).

There have been many attempts to understand the hysteresis phenomenon theoretically and numerically [2–12] and also experimentally [13]. Rao, Krishnamurthy, and Pandit have studied hysteresis extensively [3] in an N component spin system in $d=3$. They use the relaxational dynamics of the O(N) model in the $N\rightarrow\infty$ limit as first discussed by Mazenko and Zannetti [14]. They apply a sinusoidally varying external field $H(t)=H_0\sin\omega t$ and study the nature of hysteresis loops $m(H)$, where m is the mean value of the spin component parallel to the direction of applied field H. Their numerical calculation yields the following two important results. (1) As $\omega\rightarrow 0$ the hysteresis loop area A scales as $H\sim H_0^{\alpha}\omega^{\beta}$, with $\alpha=0.66\pm0.05$ and $\beta=0.33\pm0.03$ and as $\omega\rightarrow\infty$, $A\rightarrow 0$ asymptotically and (2) as ω is increased from zero, there is a symmetry breaking at a critical frequency $\omega=\omega_c(H_0)$ where the average of the magnetization $m(H)$ over one cycle of H acquires a nonzero value

$$\int_0^T m(t)dt=0 \quad \text{for } \omega<\omega_c(H_0)$$

and

$$\int_0^T m(t)dt\neq 0 \quad \text{for } \omega>\omega_c(H_0)\ ,$$

where $T=2\pi/\omega$ is the time period of one cycle of the external field. They term the result (2) a dynamic phase transition at $\omega=\omega_c(H_0)$. However, Dhar and Thomas [4] pointed out that Rao, Krishnamurthy, and Pandit ignored the possibility of a nonzero transverse magnetization in the steady state solution. They argue that the direction in which spins align need not necessarily be parallel to the external field for large ω. Dhar and Thomas take this possibility of nonzero transverse magnetization into account by taking a δ-function spin-spin autocorrelation of the transverse components in q space at $q=0$. They thereby show that there is no symmetry breaking result (2) of Rao, Krishnamurthy, and Pandit. However, for large $\omega>\omega_c'(H_0)$, the transverse spin components acquire finite nonzero (squared) average values. This result they call a dynamic phase transition in the O($N\rightarrow\infty$) model at $\omega=\omega_c'(H_0)$. Dhar and Thomas further show that as $\omega\rightarrow 0$, the hysteresis loop area scales as

*Present address: Department of Physics, Banaras Hindu University, Varanasi 221 005, Uttar Pradesh, India.

in the case of Rao, Krishnamurthy, and Pandit but with $\alpha=\beta=\frac{1}{2}$ with some logarithmic corrections. Also, as ω increases, for example, between $\omega\sim0.02$ and 0.2, they find $\alpha=0.66$ and $\beta=0.34$. It appears that these exponents vary continuously as ω varies and in the limit $\omega\to0$ they each equal $\frac{1}{2}$.

Rao, Krishnamurthy, and Pandit also do a Monte Carlo (MC) simulation [3] for the Ising ferromagnet with nearest neighbor interaction in $d=2$. This MC work was extended by Lo and Pelcovits [5] to a larger system size. Lo and Pelcovits find a dynamical phase transition as observed by Rao, Krishnamurthy, and Pandit. Also, they find a similar power-law scaling behavior for the hysteresis loop area A, but with exponents $\alpha=0.46$ and $\beta=0.36$ in their $d=2$ Ising-model simulation on a 140×140 lattice. Acharyya and Chakrabarti do a similar simulation [6] using the standard Metropolis algorithm in $d=2$, 3, and 4. They fit the hysteresis loop area for a wide range of ω, H_0, and temperature in a functional scaling form which reduces to the power law as $\omega\to0$, giving the values $\alpha=0.37$ and $\beta=0.36$ in $d=2$. They too observe a dynamical phase transition like Rao, Krishnamurthy, and Pandit. Sengupta, Marathe, and Puri [8] find exponents close to those of Lo and Pelcovits in their cell-dynamical calculation for a $d=2$ Ising system. However, Sengupta, Marathe, and Puri do not report a dynamical phase transition.

Tomé and Oliveira do a mean-field calculation for the kinetic (ferromagnetic) Ising model [7], where the system is allowed to obey Glauber stochastic dynamics. They too find a dynamic phase transition similar to that of Rao, Krishnamurthy, and Pandit. Further, a deterministic one parameter dynamical calculation was done by Jung, Gray, and Roy in a Landau m^4 potential, where m is the order parameter, for a sinusoidally varying external field [9]. Their mean-field calculation yields a power-law scaling relation with $\alpha=\beta=\frac{2}{3}$.

From the above one concludes that in the ferromagnetic Ising system, when driven by a sinusoidally varying external field, the resulting hysteresis loops show the following behavior. (1) The hysteresis loop area shows power-law scaling behavior as $\omega\to0$, and (2) the loops undergo a dynamic phase transition of the type reported by either Rao, Krishnamurthy, and Pandit or Dhar and Thomas. However, in all these systems, $O(N\to\infty)$ model included, the hysteresis loop area increases initially with ω and decreases at large ω: $A\to0$ as $\omega\to\infty$. Thus the hysteresis loss shows a peak at intermediate ω.

Quite apart and different from the treatments described above to understand hysteresis, Agarwal and Shenoy [10], following Skripov and Skripov [11] and Gilmore [12], based their work on the idea of competition among various time rates. Though the idea is quite general and could be applied to many component order parameter systems, they study hysteresis, considering only a one component uniform order parameter m with a linearly varying external field $h(t)=h_0+\dot{h}t$, $\dot{h}=$const. This simplification, though it neglects order parameter fluctuations, clearly brings out the essence of rate-competition ideas to explain hysteresis using the first-passage time (FPT) formalism [15]. They consider hysteresis to appear in the process of order parameter transition between two states separated by an energy barrier. The transition is aided by stochastic fluctuations and the relative stability of the two states is controlled by a linearly varying external field $h(t)$ given that the other parameters are fixed. The two other time scales apart from the constant $\dot{h}^{-1}$ are (1) the relaxation time T_r of the state the system occupies and (2) its decay time τ_{decay} to the other state. If the free energy is represented by the double-well Landau potential,

$$\Phi(m)=\frac{-a}{2}m^2+\frac{b}{4}m^4-h(t)m\ , \tag{1}$$

where a and b are positive constants, as adopted by Agarwal and Shenoy [10], Mahato and Shenoy [16], and the present work, T_r is related to the curvature at the minimum $m=\bar{m}_1$ (Fig. 1) of the well representing the state the system occupies, and τ_{decay} is identified [12] with the mean first-passage time (MFPT) $T_P=\langle\tau\rangle$ of passage to $m=\bar{m}_2$ (Fig. 1). Agarwal and Shenoy [10(a)] and Shenoy and Agarwal [10(b)] improve upon the physically intuitive "hysteresis criteria,"

$$T_r^{-1}>\dot{h}$$

and (2)

$$\dot{h}\geq\tau_{\text{decay}}^{-1}\ ,$$

as stated by Gilmore [12] and also by Skripov and Skripov [11]. The improved criteria [10(b)]

$$T_r^{-1}\left[\frac{\partial\ln(\bar{m}_1)}{\partial h}\right]^{-1}>\dot{h}$$

and (3)

$$\dot{h}\geq\left|\frac{\delta\Phi/D}{\delta h}\right|^{-1}\left[T_{P\downarrow}^{-1}(h)-T_{P\uparrow}^{-1}(h)\right]\ ,$$

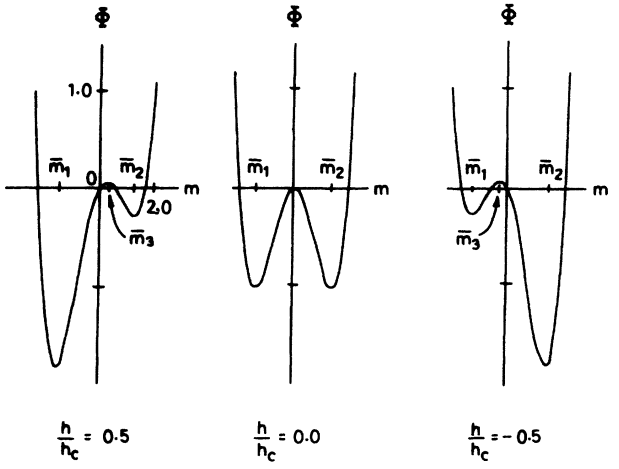

FIG. 1. Plot of m^4-Landau potential Eq. (1) with $a=2.0$, $b=1.0$ for three values of $h=0.5h_c$, 0, and $-0.5h_c$. The positions of the minima $\bar{m}_1$ and $\bar{m}_2$ and the peak $\bar{m}_3$ of the barrier are indicated on the m axis.

where $\downarrow$ and $\uparrow$ denote passage from $\overline{m}_1$ to $\overline{m}_2$ and vice versa, respectively, take into account the variation of $\Phi(m)$ with $h(t)$.

Mahato and Shenoy [16] solve the overdamped Langevin equation

$$\frac{\partial m}{\partial t} = -\frac{\delta \Phi(m)}{\delta m} + \hat{f}(t) , \tag{4}$$

for the time evolution of order parameter m. $\hat{f}(t)$ is the Gaussian white noise with the following statistics:

$$\langle \hat{f}(t) \rangle = 0 ,$$

and (5)

$$\langle \hat{f}(t)\hat{f}(t') \rangle = 2D\delta(t-t') ,$$

where the average $\langle\ \rangle$ is taken over the distribution of the noise and D is the noise strength representing the diffusion constant. Mahato and Shenoy [16] find the distribution $\rho(\tau)$ of the FPT, τ, which directly gives the jump distribution $\rho(h_J)$ in terms of the field value $h_J = h(\tau)$. They calculate the hysteresis loop from the jump distribution and hence the hysteresis loop area as a function of $\dot{h}$ and D. Apart from verifying the hysteresis criteria of Agarwal and Shenoy [10(a), 10(b)] they obtain the following results. The hysteresis loop area A does not follow any universal power-law scaling with $\dot{h}$ (analogous to ω in the sinusoidal case). However, the slopes of the log-log plot of A versus $\dot{h}$ depend on the values of D. The work of Mahato and Shenoy, however, failed to see the intuitively correct behavior of having a peak in the hysteresis area curve as $\dot{h}$ varies from 0 to ∞. This is because Mahato and Shenoy let $h(t)$ vary linearly and continued the variation till a "jump" occurred without allowing for a change of sign of the slope $\dot{h}$. As a result, the hysteresis loop area increases monotonically with $\dot{h}$. In the present work we rectify these shortcomings by considering a symmetrical sawtooth field sweep [Fig. 2(a)]

$$h(t) = (-1)^{n-1} h_0 + (-1)^n \dot{h} t' , \tag{6}$$

where $t = (n-1)/T + t'$ $(0 \le t' < T/2)$, $T = 4h_0/\dot{h}$ is the period of variation of $h(t)$, and $n = 1,2,\ldots$ is the half-period index. We expect this choice of the field sweep, apart from satisfying the spirit of the rate-competition ideas, to be closer to the sinusoidally varying field sweep used by other workers.

In the present work we vary h_0, $\dot{h}$, and D independently of one another. For small $\dot{h}$, $\dot{h} \to 0$, and for given h_0 and D the jump distribution is expected to be confined within $t = 0$ and $t = T/2$; hence we do not expect the results to be any different from the results obtained by Mahato and Shenoy for $\dot{h} \to 0$. Therefore the hysteresis loop area is not expected to follow any universal power-law behavior as $\dot{h} \to 0$ even for a symmetrical sawtooth field sweep (6). For given h_0 and D as $\dot{h}$ is increased, the FPT distribution $\rho(\tau)$ spreads beyond $t = T/2$ and subsequently even beyond $t = T$ and thus shows more than one peak, as shown in Fig. 2(b). The normalized distribution $\rho(\tau)$ contains all the information needed to obtain the hysteresis loop that confines itself within $-h_0$ and h_0. To obtain the hysteresis loop, $\rho(\tau)$ is folded into $\rho(h_J(\tau))$ as shown in Fig. 2(c). It should, however, be noted that the definition of hysteresis loop becomes different from earlier ones [3–8]. In the case of $O(N+\infty)$ model [3,4] or ferromagnetic Ising model simulations [5–8] the magnetization continuously changes as the field is varied. However, in our case of FPT formalism a change in the order parameter m (and hence magnetization) is not considered unless a jump $\overline{m}_1$ to $\overline{m}_2$ has occurred. For a jump to occur, however, the field sweep may have to undergo many (cyclic) periods. Thus the hysteresis loop obtained in our case differs from that of others at the level of the definition itself, and the occurrence of a dynamic phase transition is thus ruled out in our analysis.

As is clear from the above, we basically calculate the

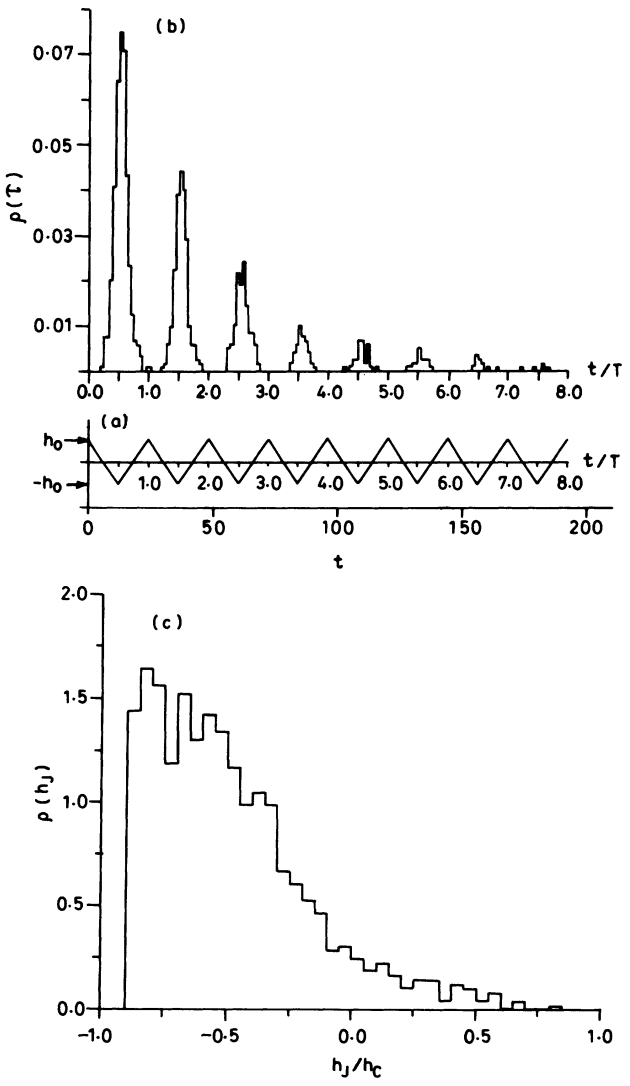

FIG. 2. (a) The field variation $h(t)$, (b) the FPT distribution $\rho(\tau)$, and (c) the corresponding jump-field distribution $\rho(h_J)$ are plotted for $h_0 = 0.9h_c$, $|\dot{h}| = 0.15h_c$, and $D = 0.6$. $\rho(\tau)$ extends up to 26 cycles of the field $h(t)$. For convenience $h(t)$ and $\rho(\tau)$ are plotted only up to eight cycles of $h(t)$. The cyclic periods $T = 4h_0/\dot{h}$ are also indicated along the $\rho(\tau) = 0$ and $h(t) = 0$ axes.

FPTs and their distribution $\rho(\tau)$ numerically in a system subjected to an external periodic field and a stochastic noise. From Fig. 2(b) we see that $\rho(\tau)$ could spread over many periods and does peak periodically, though the peaks gradually reduce in magnitude as time becomes large. The periodic nature of $\rho(\tau)$ led us to examine the recently discovered phenomenon of stochastic resonance. Benzi, Sutera, and Vulpiani [17] coin this term as they examine the possibility of a cooperative effect between the internal mechanism (stochastic noise included) and the external periodic forcing, and a consequent marked increase in response to the periodic forcing at certain stochastic noise strengths in a given dynamic system. They use the phenomenon of stochastic resonance to explain the periodic occurrence of ice ages on earth. This phenomenon has been observed in the hysteretic Schmitt electronic trigger circuit by Fauve and Heslot [18] and more importantly in a two-mode (dye) ring laser experimentally by McNamara, Wiesenfeld, and Roy [19]. Subsequently there have been many efforts to explain the phenomenon theoretically [20–22] and also many attempts to observe it in analog and numerical simulation experiments [23,24]. The sharpness and position of $\rho(\tau)$ peaks in our numerical experiment are reflected in the hysteresis loop area. We find the variation of the hysteresis loop area, for given field-sweep rates $\dot{h}$, with the noise strength D. We find the hysteresis loop area A to peak as D is increased from small $D\sim 0$ to large D. The result is a signature of the occurrence of stochastic resonance as remarked by Gage and Mandel [13]. It should be recalled that $\rho(\tau)$ represents the response (signal) to the external periodic field $h(t)$ at a given noise strength. Further, as will be explained in detail below, $\rho(\tau)$ [and equivalently $\rho(h_J)$] determines the nature of the hysteresis loop; the hysteresis loss (area of the loops) therefore plays the role of signal-to-noise ratio in the study of stochastic resonance. Our results can be verified by a very important and recently developed technique of Simon and Libchaber [25] to be discussed further in Sec. IV.

The main results that we obtain are thus that (1) the hysteresis loop area shows a peak as $\dot{h}$ increases ($A\to 0$ as $\dot{h}\to 0$ and also as $\dot{h}\to\infty$) without showing any dynamic phase transition and (2) for a given h_0 and $\dot{h}$, A shows a peak as D is increased from $D\sim 0$ to D large. As will be explained in Sec. III, this happens because, as the system is driven by a periodic field, the probability of passage over the potential barrier gets enhanced [with sharp and periodic but damped $\rho(\tau)$] only at a suitable noise strength. With stochastic noise strength below or above that particular value, the sharpness of $\rho(\tau)$, respectively, gets reduced or fuzzy. In Sec. II we briefly explain our numerical method. The results will be presented in Sec. III in detail and subsequently we discuss our results in the last section.

II. THE NUMERICAL METHOD OF LANGEVIN DYNAMICS

As mentioned earlier this work is an extension of the work of Mahato and Shenoy [16] and the details of the numerical procedure are described in Ref. [16(b)]. In this work we take a symmetrical sawtooth field sweep as given by Eq. (6) and shown in Fig. 2(a), instead of a monotonically varying linear sweep. Of course, the magnitude of the slope $|\dot{h}|$ is the same in both cases of increasing as well as decreasing $h(t)$. $|\dot{h}|$ is kept constant for simplicity and convenience, as we are interested in rate-competition ideas. We begin the field sweep at $t=0$ with $h(0)=h_0$ (>0) and the initial state is represented by the lowest minimum $m=\overline{m}_1$ ($t=0$) of the potential well (1). The Langevin equation (4) is solved using a fourth order Runge-Kutta method with adaptive step size [26]. $\hat{f}(t)$ is obtained from a Gaussian distribution of random numbers, called after every $t=t_n=n\Delta$ ($n=0,1,2,\ldots$) and kept fixed between t_n and t_{n+1}. Δ is chosen to be 0.001 (Appendix of Ref. [16(b)]). The numerical integration is continued till $m=\overline{m}_2(\tau)$, the minimum of the other well of the potential, is reached for the first time. $m(t)$ is a stochastic process and consequently the FPT, τ, is stochastic. We obtain the distribution $\rho(\tau)$ of τ by repeating the above procedure N ($=500$ typically, but taken suitably depending on $\dot{h}$, D, and h_0) times, beginning each time with a different seed value for the random numbers. To obtain sensible results we restrict to $|h_0|<h_c$ the critical field where one of the two wells of the potential (1) disappears. Throughout our calculation we have taken $a=2.0$ and $b=1.0$ for convenience. The distribution $\rho(\tau)$ is then folded up to transform into $\rho(h_J)$, $h_J=h(\tau)$; h_J is restricted to $-h_0\le h_J\le h_0$ [Fig. 2(c)]. From $\rho(h_J)$ the "magnetization" is obtained as

$$\frac{M(h_J)}{h_c}=1-\frac{2}{h_c}\int_{h_J}^{h_0}\rho(h_J')dh_J' , \tag{7}$$

where the saturation magnetization is taken to be ± 1 (in units of h_c). Equation (7) gives the upper branch of the hysteresis loop and the lower branch is obtained by symmetry. It follows that the hysteresis loop area has an upper bound of $4h_0h_c$. Further, since $\rho(h_J)$ is obtained from $\rho(\tau)$ which may spread over many periods of $h(t)$, the hysteresis loop area

$$A=\oint M(h_J)dh_J \tag{8}$$

cannot be interpreted as hysteresis loss over one cycle of the field sweep. A is the hysteresis loss over the entire process of passage from one state to the other of a large ensemble of systems (Sec. IV) and the process is completed over many cycles of this field sweep.

Numerical errors in evaluating the hysteresis loop area come at various stages of calculation right from the integration of the Langevin equation to obtain the FPT τ. There are two main sources of error in evaluating τ: (1) the time discretization procedure and (2) the integration of Eq. (4) with constant $\hat{f}(t)$. We have used standard routines and the function to be integrated is very well behaved; thus the error (2) is quite small. The error (1) is kept within only a few percent (Appendix of Ref. [16(b)]) by taking $\Delta=0.001$, over which $\hat{f}(t)$ remains constant. Another source of error that could crop up in our calculation is in the averaging of the stochastic quantities.

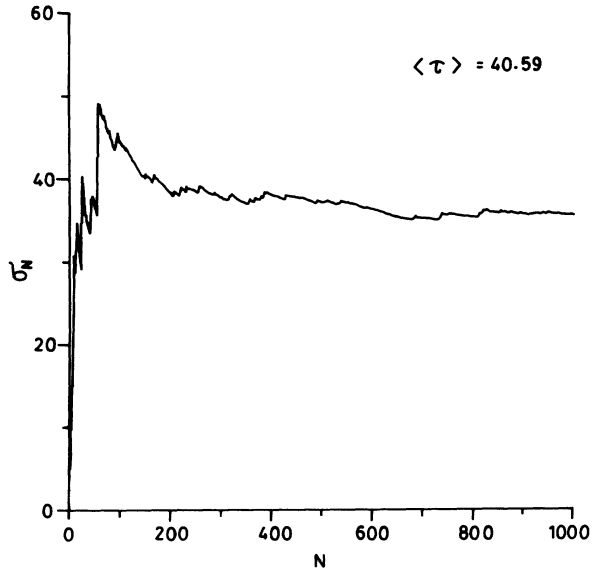

FIG. 3. Standard deviation σ_N of the mean FPT with the number of runs N for Fig. 2 is plotted. For comparison the mean FPT with $N=1000$ is 40.6.

This error is minimized by taking a large number of runs and checking the standard deviation of the mean FPT. The plot of standard deviation σ_N with N number of runs is shown in Fig. 3. As is evident σ_N gets stabilized (fluctuations are confined to a sensible limit) and is of the order of the mean FPT, as it should be. With careful numerical evaluation we are confident of our results being qualitatively correct if not quantitatively exact. We present our results in the following section.

III. NUMERICAL RESULTS

A. Variation of hysteresis loop area with field sweep rate and amplitude

In order to investigate the variation of the hysteresis loop area with the field sweep rate $\dot{h}$ we keep h_0 and D fixed. For small $\dot{h}$ $\rho(\tau)$ remains confined to the first half cycle of the field sweep $h(t)$ and the hysteresis loops show saturation (Fig. 4). It is to be noted, however, that the lower branch of the hysteresis loop is obtained by symmetry. As $\dot{h}$ is increased $\rho(\tau)$ spreads up to and then beyond $\tau=T/2$, where $T=4h_0/\dot{h}$ is the period of one cycle of the $h(t)$ sweep. The saturation effect shown in Fig. 4 thus disappears as jump values of h_J continue till $h(t)=-h_0$. On further increase of $\dot{h}$, $\rho(\tau)$ spreads to more than one period. $\rho(\tau)$, however, peaks close to $t=(2n-1)T/2$, where $n=1,2,\ldots$ is the half-cycle index of $h(t)$, and more and more jumps take place close to $h=-h_0$. Figures 5 and 6 show $\rho(\tau)$ and the corresponding hysteresis loops at two values of $\dot{h}$. Beyond a certain value of $\dot{h}$, however, the $\rho(\tau)$ peaks gradually start becoming broader and broader and therefore the jumps take place almost all over between $-h_0$ and h_0, thereby reducing the hysteresis loop area (Fig. 7).

The nature of the distribution $\rho(\tau)$ can be explained thus. When $\dot{h}$ is small, the system had enough time to decay from $m=\bar{m}_1(0)$ to $m=\bar{m}_2(\tau)$ before $t=T/2$ [Fig. 4(a)]. However, as $\dot{h}$ is increased, that is, $T=4h_0/\dot{h}$ decreased, the system cannot decay completely before $t=T/2$ and it continues to decay even beyond $t=T/2$. $\rho(\tau)$ remains broad. When $\dot{h}$ is increased still further, since the barrier height becomes smallest at $t=(2n-1)T/2$, passages take place around these values of t. If the system fails to cross over the barrier, say, around $t=(2n-1)T/2$, it waits for its next chance around $t=(2n+1)T/2$. However, as $\rho(\tau)$ spreads to many cycles initially the peaks around $t=(2n+1)T/2$ gradually become narrower, that is, jumps cluster around $h=-h_0$, and the hysteresis loop area becomes larger. When $\dot{h}$ is made still larger, the number of $\rho(\tau)$ peaks increases but the peaks begin to widen (Fig. 7). This is because after the system crosses the peak of the potential barrier it takes some time to roll down to $m=\bar{m}_2$, but by that time $h(t)$ moves away from $-h_0$. In the extreme case the peaks overlap and the area $A\to 0$. This situation comes at large $\dot{h}$ depending on the values of D and h_0.

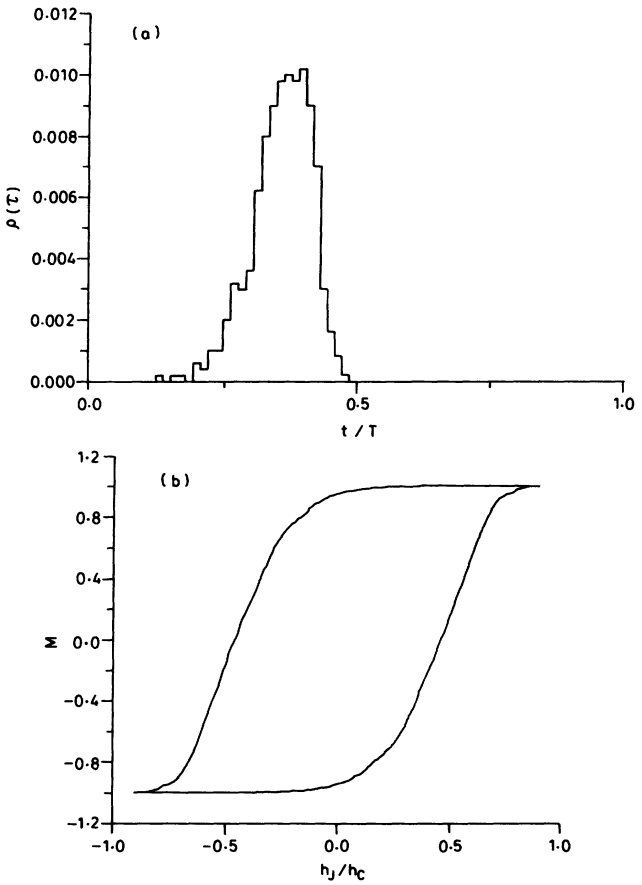

FIG. 4. (a) The FPT distribution $\rho(\tau)$ and (b) the corresponding hysteresis loop are plotted for $h_0=0.9h_c$, $|\dot{h}|=0.005h_c$ $D=0.4$ in 500 runs. The positions of the half cyclic periods $T/2$ are indicated along the time axis. Notice that $\rho(\tau)$ is confined within $t=T/2$.

A typical plot of hysteresis loop area versus $\dot{h}$ is shown in Fig. 8. The qualitative nature of this plot is similar to what others find [3–8]. However, as noted earlier, except for small $\dot{h}$, to obtain a hysteresis loop we need to cycle the field many times and that is how hysteresis is defined here. This is very much in contrast to the hysteresis loop obtained for each cycle of the field sweep in the case of other workers.

As mentioned in Sec. II the hysteresis loop area has an upper bound of $4h_0h_c$. Therefore for larger h_0, it is reasonable to expect the possibility of finding a larger hysteresis loop area for any fixed value of $\dot{h}$. We repeated our calculation with different h_0. The curve with (0) points in Fig. 8 is the hysteresis loop area versus $\dot{h}$ for $h_0=0.5h_c$. It is to be noticed that, as expected, the peak of area A versus $\dot{h}$ shifts to a lower value of $\dot{h}$ for smaller h_0. This is because, for small h_0, the period $T=4h_0/\dot{h}$ for a given $\dot{h}$ is scaled down compared to that for larger h_0 and hence $\rho(\tau)$ peaks start broadening at smaller values of $\dot{h}$ than is the case for larger h_0. Again, as expected for a given $\dot{h}$ and D the hysteresis loop area increases monotonically with h_0, as shown in Fig. 9.

B. Variation of hysteresis loop area versus D and the phenomenon of stochastic resonance

The diffusion constant D is defined in Eq. (3). D determines the sharpness of the Gaussian distribution of the noise $\hat{f}(t)$ about zero; in other words, it determines and is proportional to the thermal fluctuation of the system. Therefore a larger D will correspond to a larger system "temperature." One would, therefore, expect that the hysteresis loop area A will be small for larger D values for given $\dot{h}$ and h_0 because it will be easier for the system to cross over the potential barrier. A plot of A versus $\dot{h}$ for various values of $D=0.3$, 0.4, 0.6, and 1.0 and fixed $h_0=0.9h_c$ is shown in Fig. 10. It is to be noticed that the above mentioned behavior is followed for small $\dot{h}$. However, for large $\dot{h}$ the area A shows just the reverse behavior, namely, A increases with D. Further, the peaks of the curves shift to larger values of $\dot{h}$ as D is increased. Therefore for intermediate $\dot{h}$ values the area shows a crossover behavior as D is changed, that is, A increases in the beginning and then starts decreasing as D is increased further. This is therefore investigated in more

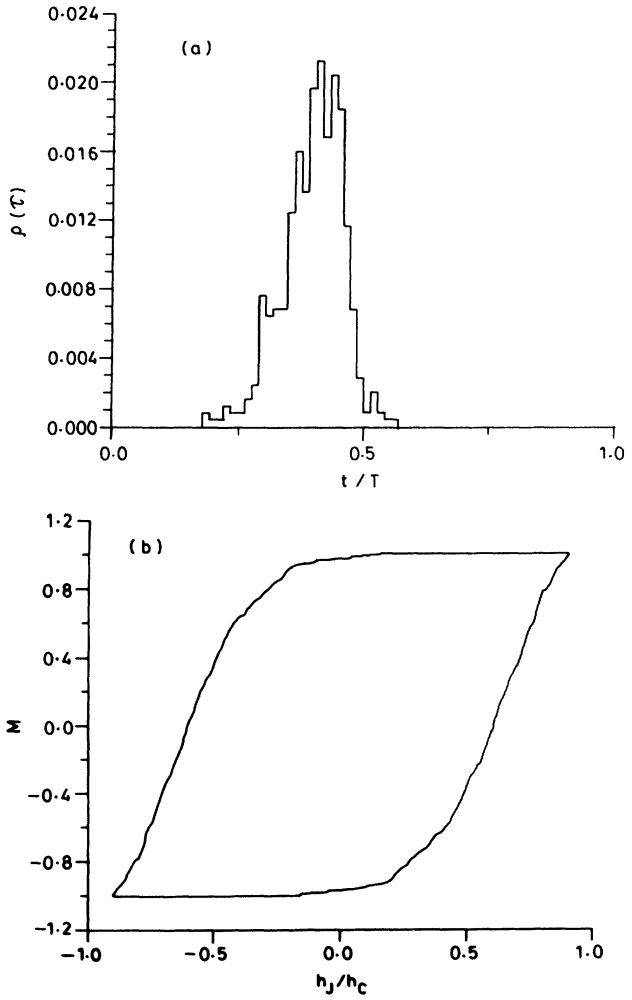

FIG. 5. Same as in Fig. 4 but with $|\dot{h}|=0.01h_c$. $\rho(\tau)$ extends beyond $t=T/2$.

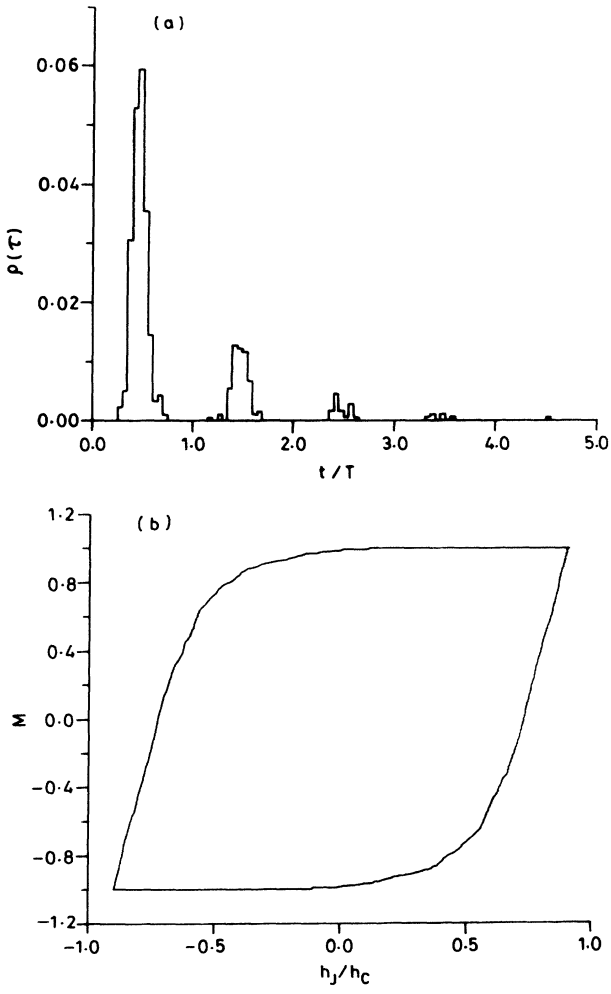

FIG. 6. Same as in Fig. 4 but with $|\dot{h}|=0.05h_c$. $\rho(\tau)$ spreads to five cycles ($t=5T$).

detail by keeping h and h_0 fixed and varying D.

Figure 11 shows the plots of the hysteresis loop area A versus the diffusion constant D. Each of these plots is analogous to Fig. 3 of Ref. [19]. This is surely an example of stochastic resonance. This behavior can be explained by carefully examining the nature of the corresponding $\rho(\tau)$. We present in Fig. 12 $\rho(\tau)$ for $\dot{h}=0.2h_c$ and $h_0=0.9h_c$ and three values of $D=0.3$, 1.0, and 2.0, corresponding, respectively, to where A is smaller than, close to, and again smaller than the peak of the A versus D curve. These distributions are similar to the ones reported by Zhou, Moss, and Jung [21]. $\rho(\tau)$ results from the competition between the D dependent passage time and the field-sweep rate $\dot{h}^{-1}$. For small values of $D=0.3$, $\rho(\tau)$ spreads over many field-sweep cycles (we reach up to a maximum of 28 cycles in 500 runs). The $\rho(\tau)$ peaks are sharp but are shifted to the right from $t=(2n-1)T/2$, $n=1,2,\ldots$ [Fig. 12(a)]. This happens because, even after the system crosses over the peak of the potential barrier close to $h(t)=-h_0$, it is unable to roll down to the bottom at $m=\overline{m}_2$ quickly enough [compared to the change of field $h(t)$] because of sluggishness caused by the small D. Therefore most of the "jumps" take place away from $-h_0$ (to the next half cycle) and hence the hysteresis loop area is small. At $D=1.0$, $\rho(\tau)$ does not spread to as many cycles (a maximum of 20 cycles in 180 runs) and the peaks are not as sharp [Fig. 12(b)]. However, even though the peaks are wide, compared to the $D=0.3$ case, they are very close to $t=(2n-1)T/2$, that is, very close to $-h_0$. In other words, most of the jumps $\overline{m}_1(0)\rightarrow\overline{m}_2(\tau)$ take place where the potential barrier height is the least (resonant situation). At large $D=2.0$, $\rho(\tau)$ gets confined to only a few cycles of $h(t)$ [Fig. 12(c)] and also the peaks seem to

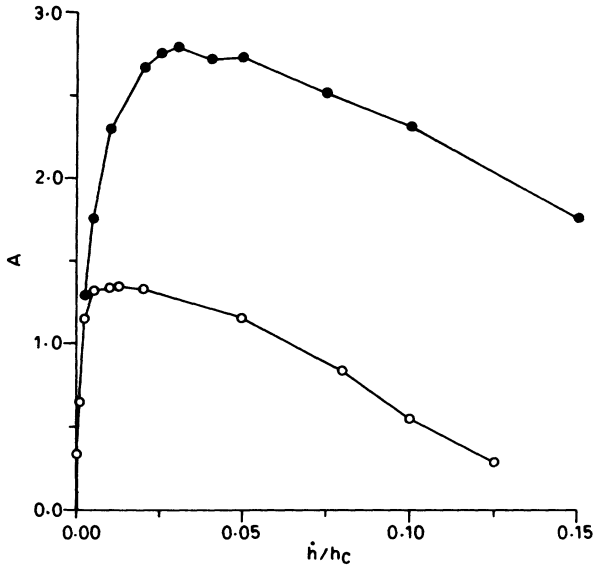

FIG. 8. Hysteresis loop area A (in units of h_c^2) versus $\dot{h}/h_c$ for $h_0=0.9h_c$ (●) and $h_0=0.5h_c$ (○) and $D=0.4$.

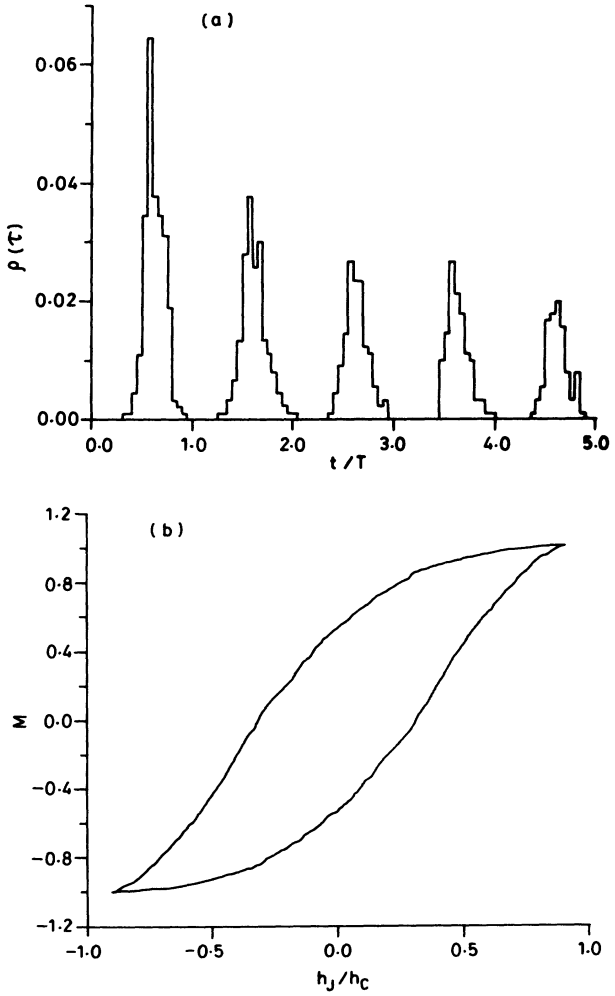

FIG. 7. Same as in Fig. 4 but with $|\dot{h}|=0.2h_c$ and the data are for 1000 runs. $\rho(\tau)$ extends to $t=28T$. $\rho(\tau)$ peaks are broader than in Fig. 6(a) and also they are shifted to the right from $(2n-1)T/2$, $n=1,2,\ldots$. Only ten periods are shown in the figure.

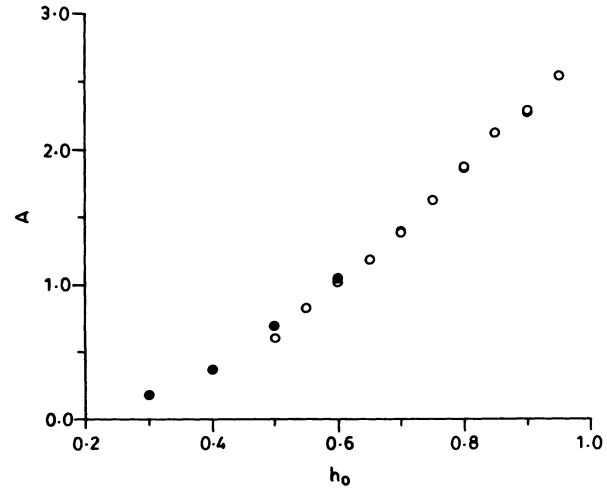

FIG. 9. Variation of hysteresis loop area A (in units of h_c^2) with h_0 for $|\dot{h}|=0.1h_c$ and $D=0.8$ (●) and 0.5 (○).

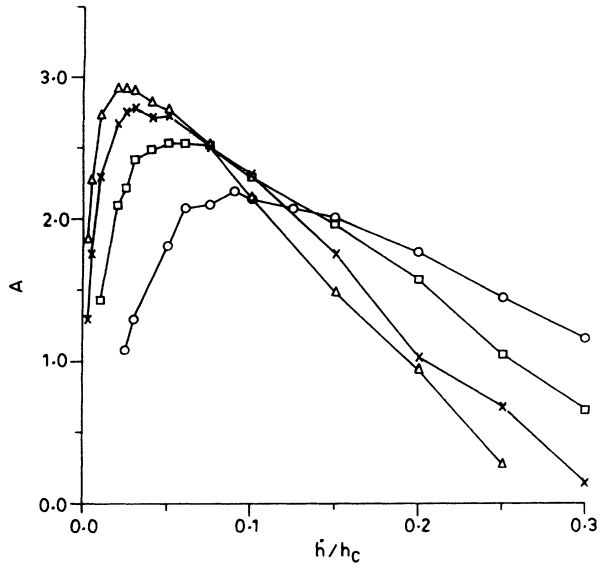

FIG. 10. Variation of hysteresis loop area A (in units of h_c^2) with $\dot{h}/h_c$ for various values of $D=0.3(\triangle)$, $0.4(\times)$, $0.6(\square)$, and $1.0\,(\circ)$ and $h_0=0.9h_c$.

occur close to $t=(2n-1)T/2$. However, the peaks are very broad and tend to overlap and even merge together. Therefore the probability of jump values away from $h=-h_0$ is considerable, thus reducing the hysteresis loop area. The corresponding hysteresis loops are shown in Fig. 13.

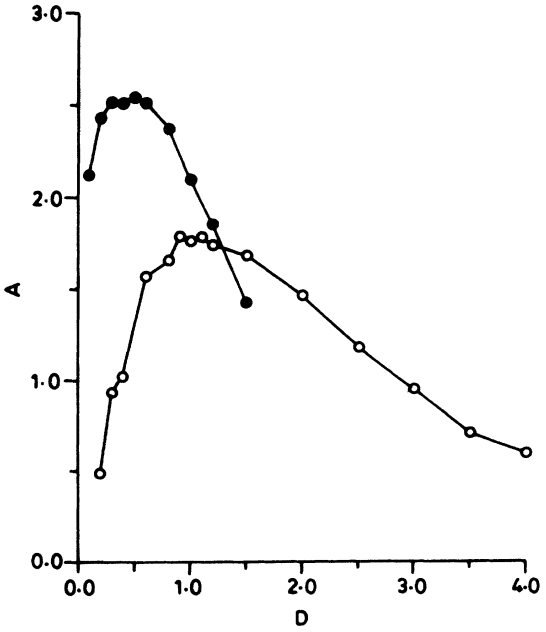

FIG. 11. Variation of hysteresis loop area A (in units of h_c^2) with D for $h_0=0.9h_c$ and two values of $|\dot{h}|=0.075h_c$ (●) and $0.2h_c\,(\circ)$.

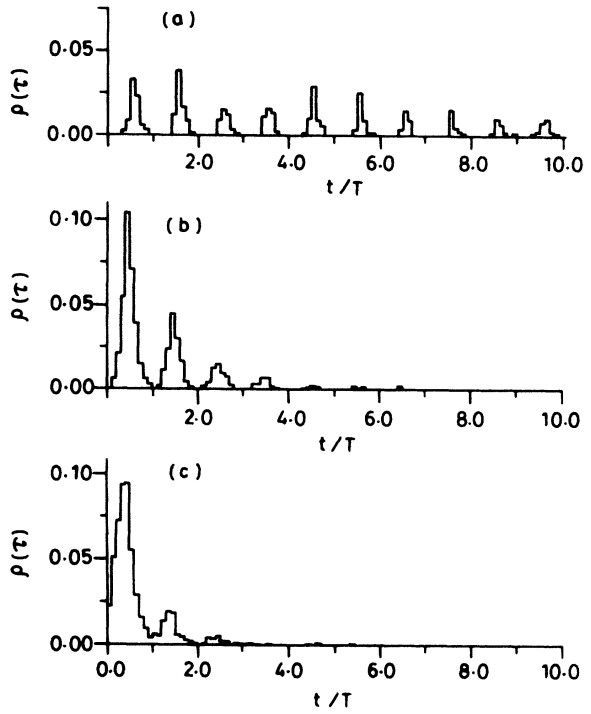

FIG. 12. Comparison of the nature of $\rho(\tau)$ for $h_0=0.9h_c$, $|\dot{h}|=0.2h_c$, and three values of $D=$(a) 0.3, (b) 1.0, and (c) 2.0. $\rho(\tau)$ for $D=0.3$ extends to 53 cycles of $h(t)$ but for convenience and better comparison only up to $t=10T$ is shown. $T=4h_0/\dot{h}$ is the period of $h(t)$. At $t=nT$ $(n=1,2,\ldots)$ marks are put on the time axis.

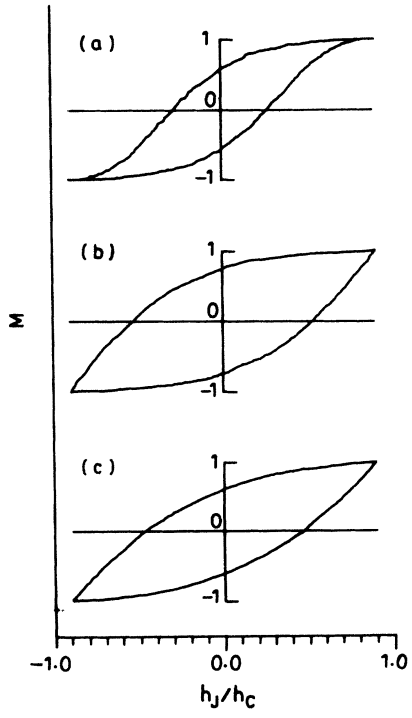

FIG. 13. Hysteresis loops for the FPT distributions $\rho(\tau)$ shown in Fig. 12 are shown for (a) $D=0.3$, (b) $D=1.0$, and (c) $D=2.0$ (M is plotted in units of h_c).

IV. DISCUSSION

The qualitative nature of the variation of the hysteresis loop area A with $\dot{h}$ is similar to that obtained by many authors [3–8] including Gage and Mandel [13], who measured hysteresis loop areas in a two-mode (dye) ring laser. In brief, the procedure for calculating the hysteresis loop area in our case is as follows. We take an ensemble of noninteracting systems each in the same state $\overline{m}_1$, in the corresponding potential well, at $t=0$. This situation is equivalent to a collection of identical noninteracting magnetic grains with their spins aligned in the direction of a uniform magnetic field. Then we observe the ensemble as the field is swept in a triangular fashion, record the time τ when a system reaches $\overline{m}_2(\tau)$ for the first time, and remove the particular system from the ensemble. We continue observation till the last surviving system of the ensemble reaches $\overline{m}_2$ of its potential well (the last grain of the magnetic system switching its direction for the first time). This gives $\rho(\tau)$ and completes the upper branch of the hysteresis loop; the lower branch is obtained by symmetry. This procedure, except for small $\dot{h}$, may require observation for more than one cycle of the field sweep. In contrast, as in the usual hysteresis experiments, other works calculate the complete loop in one cycle of the field sweep and averaging is done over many cycles just to remove the fluctuations introduced in the measurement process, etc. [3–8,13]. Therefore the comparison of Fig. 8 with the results of others is not reasonable. Even otherwise we do not claim to reproduce even qualitatively all the hysteresis behavior seen by others. For example, our procedure does not allow us to see the dynamic phase transition seen by all the workers in Ising-model systems [3–8] and also indirectly by Gage and Mandel in the two-mode (dye) ring laser [13]. Gage and Mandel perform their experiment at fixed frequency of the modulation of the pump-parameter asymmetry at various mean pump-parameter values. The mean pump-parameter value determines the height of the potential barrier (of the two-well potential), effectively changing the mean FPT $\langle\tau\rangle$. If we think in terms of a fixed potential form at given D, effectively they performed the experiment at a different relative frequency ω. With this interpretation their results show the same qualitative behavior of A versus ω. Interestingly, Gage and Mandel's results qualitatively support the second of the rough hysteresis criteria (2) given in the Introduction.

Gage and Mandel [13] observe that the study of the hysteresis cycle is a convenient technique for exhibiting stochastic resonance. This fact has been very clearly brought out in our numerical experiment, which is very similar to the theoretical and analog simulation results of Zhou, Moss, and Jung [21]. Interestingly, the shift of the $\rho(\tau)$ peaks to the right of $t=(2n-1)T/2$ in Fig. 12(a) for small D is a similar effect shown in Fig. 2 of Ref. [13]. This shift is responsible for the hysteresis loop area being small.

Recently a very ingenious experiment has been devised by Simon and Libchaber to directly observe the Kramers escape rate in a two-well potential system [25]. Our numerical work is closest to what they study, namely, the escape rate distribution $\rho(\tau)$. In that experiment also backward passage is not studied. They also seek to verify the occurrence of stochastic resonance. They report that they find no evidence of stochastic resonance in their experiment. This is very surprising. The distribution $\rho(\tau)$ they observe is very similar to what we get. The present authors contend that with a little careful analysis and a further observation of $\rho(\tau)$ with a wider range of noise strength Simon and Libchaber's experiment [25] will yield stochastic resonance. Figures 10 and 11 provide an important hint that to observe stochastic resonance at low frequencies one needs to do the experiment at a low noise strength. Figure 10 (fixed $\dot{h}/h_c$ and variation of A in the space of D) indicates the limits of the range of $\dot{h}$ (or the frequency in the case of the external sinusoidal field) within which stochastic resonance can be observed for a given range of D values. Our numerical work, however, corroborates many aspects of the $\rho(\tau)$ observed by Simon and Libchaber.

ACKNOWLEDGMENTS

A part of this work was carried out in the Department of Physics, Banaras Hindu University (BHU). M.C.M. thanks Y. Singh for discussion and BHU for providing all the necessary facilities to complete the work. Financial support from the Council of Scientific and Industrial Research, India is gratefully acknowledged.

[1] (a) J. A. Ewing, Proc. R. Soc. London **46**, 269 (1889); (b) C. P. Steinmetz, Trans. Am. Inst. Electr. Eng. **9**, 3 (1992).

[2] (a) J. A. Barker, D. F. Schreiber, B. G. Huth, and D. E. Everett, Proc. R. Soc. London Ser. A **38b**, 251 (1983); (b) I. D. Mayergoyz, Phys. Rev. Lett. **56**, 1518 (1986).

[3] M. Rao, H. R. Krishnamurthy, and R. Pandit, Phys. Rev. B **42**, 856 (1990); J. Phys. Condens. Matter **1**, 9061 (1991).

[4] D. Dhar and P. B. Thomas, J. Phys. A **25**, 4967 (1992).

[5] W. S. Lo and R. A. Pelcovits, Phys. Rev. A **42**, 7471 (1990).

[6] M. Acharyya, B. K. Chakrabarti, and A. K. Sen, Physica A **186**, 231 (1992); M. Acharyya and B. K. Chakrabarti, *ibid.* **192**, 471 (1993).

[7] T. Tomé and M. J. de Oliveira, Phys. Rev. A **41**, 4251 (1990).

[8] S. Sengupta, Y. J. Marathe, and S. Puri, Phys. Rev. B **45**, 7828 (1992).

[9] P. Jung, G. Gray, and R. Roy, Phys. Rev. Lett. **65**, 1873 (1990).

[10] (a) G. S. Agarwal and S. R. Shenoy, Phys. Rev. A **23**, 2719 (1981); (b) S. R. Shenoy and G. S. Agarwal, *ibid.* **29**, 1315 (1984); (c) K. P. N. Murthy and S. R. Shenoy, *ibid.* **36**, 5087 (1987).

[11] V. P. Skripov and A. V. Skripov, Usp. Fiz. Nauk **128**, 193

(1979) [Sov. Phys. Usp. **22**, 389 (1979)].
[12] R. Gilmore, Phys. Rev. A **20**, 2510 (1979).
[13] E. C. Gage and L. Mandel, J. Opt. Soc. Am. B **6**, 287 (1989).
[14] G. Mazenko and M. Zannetti, Phys. Rev. B **32**, 4565 (1985).
[15] R. Stratonovich, *Topics in the Theory of Random Noise,* translated by R. A. Silverman (Gordon and Breach, New York, 1963), Vol. 1, Chap. 4.
[16] (a) M. C. Mahato and S. R. Shenoy, Physica A **186**, 220 (1992); (b) J. Stat. Phys. **73**, 123 (1993).
[17] (a) R. Benzi, A. Sutera, and A. Vulpiani, J. Phys. A **14**, L453 (1981); (b) R. Benzi, G. Parisi, A. Sutera, and A. Vulpiani, SIAM J. Appl. Math. **43**, 565 (1983).
[18] S. Fauve and F. Heslot, Phys. Lett. **97A**, 5 (1983).
[19] B. McNamara, K. Wiesenfeld, and R. Roy, Phys. Rev. Lett. **60**, 2626 (1988).
[20] B. McNamara and K. Wiesenfeld, Phys. Rev. A **39**, 4854 (1989).
[21] T. Zhou, F. Moss, and P. Jung, Phys. Rev. A **42**, 3161 (1990).
[22] C. R. Doering and J. C. Gadoua, Phys. Rev. Lett. **69**, 2318 (1992).
[23] L. Gammaitoni, F. Marchesoni, E. M. Saetta, and S. Santucci, Phys. Rev. Lett. **62**, 349 (1989).
[24] G. Vemuri and R. Roy, Phys. Rev. A **39**, 4668 (1989).
[25] A. Simon and A. Libchaber, Phys. Rev. Lett. **68**, 3375 (1992).
[26] W. H. Press, B. P. Flennery, S. A. Teukolsky, and W. T. Vetterling, *Numerical Recipes* (Cambridge University Press, Cambridge, England, 1987).